ORIGINAL RESEARCH

Optimized Modeled Myofascial Release Enhances Wound Healing in 3-Dimensional Bioengineered Tendons: Key Roles for Fibroblast Proliferation and Collagen Remodeling

Manal Zein-Hammoud, PhD, and Paul R. Standley, PhD

ABSTRACT

Objective: The purpose of this study was to evaluate the mechanisms of action of optimized myofascial release (MFR) on wound healing using a 3-dimensional human tissue construct.

Methods: Bioengineered tendons were cultured on a deformable matrix, wounded using a steel cutting tip, then strained in an acyclic manner with a modeled MFR paradigm at 103% magnitude for 5 minutes. Imaging and measurements of the width and wound size were performed daily, and the average tissue width of the entire bioengineered tendon was measured, and wound size and major and minor axes of the elliptical wound were additionally measured. Assessments of actin and collagen were performed by immunofluorescence, and Gomori's trichrome staining and fibroblast nuclei deposition was quantified using the CellProfiler analysis software.

Results: Optimized modeled MFR treatment significantly reduced the wound size and increased both collagen density and cell deposition at the wound site. All measures of wound healing improvements required the presence of proliferating fibroblasts.

Conclusion: Myofascial release—induced cell deposition and collagen density at wound sites required actively proliferating fibroblasts. If clinically translatable, our results support a mechanism by which MFR improves patient wound healing. (J Manipulative Physiol Ther 2019;42:551-564)

Key Indexing Terms: *Fibroblasts; Stress, Mechanical; Wound Healing*

INTRODUCTION

Myofascial release (MFR) is one of the most commonly used manual medicine treatments designed to stretch and elongate the fascia and underlying soft tissue to release areas of decreased fascial motion.[1,2] Documented results show that MFR reduces swelling and inflammation, improves alignment and range of motion and systemic blood flow, attenuates myofascial pain, enhances wound healing, and improves physical performance.[3,4] Fibroblasts, the primary cell type in connective tissue such as fascia, play a critical role in wound healing and regulation of the local inflammatory response.[5,6] In addition, fibroblasts respond to mechanical stimuli leading to gene expression modifications and therefore are considered a logical target for MFR treatment.[1,2,7] Despite these reported clinical outcomes, little is known about the mechanisms underlying the efficacy of MFR. We have previously used both 2-dimensional and 3-dimensional (3D) fibroblast tissue constructs to identify potential mechanisms that may explain clinical efficacies of MFR.[1,2,8] Our results from the 2-dimensional fibroblast construct studies showed that modeled MFR applied in vitro inhibits fibroblast cytotoxic effects and induces expression of various anti-inflammatory and growth factors.[1,2] The 3D bioengineered tendon (BET) is an improvement upon the 2-dimensional scratch wound model, and therefore was used as a vital biomechanical feedback system that dictates signaling and adaptive response in wound repair.[9]

Department of Basic Medical Sciences, University of Arizona, College of Medicine, Phoenix, Arizona.

Corresponding author: Paul R. Standley, PhD, Department of Basic Medical Sciences, University of Arizona, College of Medicine, 435 N 5th Street, Phoenix, AZ 85004.
(e-mail: *standley@email.arizona.edu*).

Paper submitted October 15, 2018; in revised form January 1, 2019; accepted January 29, 2019.

0161-4754

https://doi.org/10.1016/j.jmpt.2019.01.001

We have previously reported differential effects of modeled MFR strain duration and magnitude, each inducing dose-dependent fibroblast responses similar to studies that assess optimal dose/duration of pharmacologics.[8] Fixing the magnitude at 6% for 5 minutes resulted in a statistically significant decrease in wound area of MFR-treated BETs compared with nonstrained, which could be attributed to changes in the extracellular matrix (eg, collagen synthesis, secretion, and architecture) and gene activation. However, optimal results were achieved when fixing the magnitude at 3% for 5 minutes' duration.[8] When the same technique was applied to fibroblast-free BETs, the desired effect was not observed, suggesting that fibroblasts are required for the wound healing process and that optimum MFR magnitude and duration are essential for achieving optimal wound healing.[8]

Therefore, the purpose of this study was to evaluate the mechanisms of action of optimized (3% for 5 minutes) MFR-induced wound healing using a 3D in vitro model. Wound healing and collagen density were analyzed and assessed in both normally grown fibroblasts and growth-arrested fibroblasts. We hypothesized that optimized MFR treatment in the presence of proliferating fibroblasts plays a critical role in wound closure. If clinically translatable, our results support a likely mechanism by which optimized MFR improves wound healing and enhances physical performance of patients.

Methods

Cell Culture and Fabrication of Bioengineered Tendons (BETs)

Commercially available normal human dermal fibroblasts were cultured at 37°C, 5% CO_2, and 100% humidity in Dulbecco's modified Eagle's medium supplemented with either 2% fetal bovine serum and 1% penicillin-streptomycin for normal growth of fibroblasts or with 0.2% fetal bovine serum and 1% penicillin-streptomycin to arrest fibroblast growth at G_0 stage of the cell cycle. The medium was replaced with fresh prewarmed growth medium every 2 days. Confluent cultures, acquired within 7 to 10 days, were passaged at a ratio of 1:3, and cell passages between 4 and 10 were used for all experiments. Collagen-fibroblast gel was created by mixing normal human dermal fibroblasts at a concentration of 1000 cells/μL in a solution of 70% PureCol collagen type I (Advanced BioMatrix, Inc) and 30% 5X Dulbecco's modified Eagle's medium. A linear Trough Loader (Flexcell International Corp), placed beneath the Tissue Train plates (Flexcell International Corp), was used to create a loading channel for the gel. The 6-well formatted plates consisted of flexible elastomeric well bottoms that were attached to nondeformable nylon mesh anchors at each end of the long axis. A cylindrical structure attached at the 2 anchors was created by adding 200 μL of the collagen-fibroblast gel to the loading channel and allowed to polymerize for 2 hours in a humidified 37°C incubator. After the gel matrix polymerized, the vacuum was released, allowing the BETs to be free from all attachments except at the 2 anchor points. Fresh culture medium supplemented with either 2% or 0.2% fetal bovine serum was then added to each well, and the BETs were allowed to acclimate for 24 to 48 hours before undergoing wounding and modeled MFR treatment.

Groups

In the whole study, we used 4 groups: nonstrained BETs cultured in 2% FBS medium (2% FBS-NS), MFR-strained BETs cultured in 2% FBS medium (2% FBS-MFR), nonstrained BETs cultured in 0.2% FBS medium (0.2% FBS-NS), and MFR-strained BETs cultured in 0.2% FBS medium (0.2% FBS-MFR). The sample size in this study ranged between 4 and 11.

BET Wounding

An artificial wound was created using a sterile stainless-steel cutting tip. This sterile device had a circular diameter of 0.75 mm and a cutting area of 0.442 mm^2. A soft cutting mat was placed directly under the tissue and held steadily with sterile forceps. The cutting tip was positioned perpendicularly to the BET and slowly pressed onto the tissue in a gentle rotating motion until the cutting tip penetrated the BET and made contact with the underlying cutting mat. The cutter was then slowly lifted away from the BET to create an area completely devoid of fibroblasts and extracellular matrix at the approximate center of the BET. Photomicrographs were captured immediately after wounding to establish a baseline wound size for each BET. Two groups of BETs were used in the study: MFR strained (treated) or NS (control).

MFR Strain Paradigm

Strain was slowly applied to elongate the tissue to 2.5% of its resting length per second to reach a maximum 3% strain (ie, to 103% of its initial resting length). The BETs were then held at 3% elongation for 5 minutes. The strain was then slowly released back to baseline at a rate of −1.5% per second. The corresponding magnitude and duration were chosen based on our previous study, where we modified the conditions to obtain optimal wound healing.[8] The NS BETs served as controls. The baseline algorithm of the in vitro MFR paradigm was determined by quantitative analysis of videomorphic recordings of clinically applied MFR.[1] The strain frequency, direction, and loading rates of the optimized MFR were applied in vitro using the Flexercell FX-4000 Tension Plus System (Flexcell International Corp). During the modeled MFR treatment, BETs were stretched uniaxially in the direction of their long axis by placing a loading post beneath the elastomeric well bottom and applying negative pressure. The pressure

increased the distances between the 2 opposite nondeformable anchors to which each BET was attached.

Analysis of Wound Area and Dimensions

Both MFR-treated and NS BETs were incubated for 6 days after treatment. Daily imaging and measurements of the width and wound size were performed at the same time each day. The average tissue width of the entire BET was measured at the center of the wound and at approximately 2 mm to the right and left of the center location using ImageJ (National Institutes of Health). Wound closure was assessed by capturing photomicrographs using an IX71 Olympus inverted microscope and DP71 camera (Olympus America Inc) immediately after wounding and MFR (day 0) and daily thereafter until day 6. Images were then converted to black and white with Adobe Photoshop CS2 version 9.0 (Adobe Systems Inc) and analyzed for changes in wound size and shape using CellProfiler analysis software (Broad Institute Imaging Platform). The CellProfiler algorithm detected the BET wound edges based on pixel tone and color, enabling the measurement of the overall wound area. The algorithm additionally quantified the length of the long (major) and short (minor) axes of the elliptical wound.

Immunofluorescence

Assessment of collagen type 1A2 and actin was performed by immunofluorescence using mouse monoclonal primary anti-collagen and mouse monoclonal anti-actin, respectively. The BET longitudinal sections (15 μm thick) were fixed by heating slides at 37° for 20 minutes, followed by washing with 1X phosphate buffer saline (PBS) (Thermo Fisher Scientific, Waltham, Massachusetts). The BETs were then blocked and permeabilized with 2% bovine serum albumin (Thermo Fisher Scientific, Waltham, Massachusetts) and 0.2% Triton X-100 (Thermo Fisher Scientific, Waltham, Massachusetts) for 1 hour. Slides were then washed with 1X PBS and incubated at 4°C overnight with primary antibodies recognizing collagen 1A2 (sc-376350, Santa Cruz Biotechnology), at a concentration of 1/50 diluted in PBS. The following day, slides were washed with PBS and incubated with secondary antibody (donkey anti-mouse IgG; NL493-conjugated antibody; R&D Systems), at a concentration of 1/200 diluted in PBS. This secondary antibody was mixed with anti-actin, α-smooth muscle-FITC clone 1A4 (F3777, Sigma Aldrich), at a concentration of 1/100 diluted in PBS. The mixture of antibodies was left on slides for 1 hour, followed by subsequent washing and mounting with Vectashield containing 4',6-diamidino-2-phenylindole (DAPI, Vector Laboratories).

Gomori's Trichrome Staining

Assessment of total collagen was determined using Gomori Trichrome stain (87020, Richard-Allan Scientific). The BET longitudinal sections (15 μm thick) were placed in a Coplin glass staining jar filled with Bouin's fluid at 56°C for 1 hour, followed by rinsing sections in running tap water for 3 to 5 minutes until yellow color disappeared. Afterward, sections were placed in Working Weigert's iron hematoxylin stain for 10 minutes, followed by rinsing in running tap water for 5 to 10 minutes. Slides were then placed in Trichrome stain for 15 minutes, followed by incubating in 1% acetic acid solution for 1 minute. Sections were then rinsed in distilled water for 30 seconds and dehydrated in 2 changes of 95% alcohol for 1 minute each. Slides were finally cleared in Xylene (MilliporeSigma, St. Louis, Missouri) for 30 seconds and mounted. Collagen was stained in blue, whereas nuclei were stained black.

Collagen Quantification

The intensity of total collagen (stained by Gomori), collagen type 1A2, and actin (stained by immunofluorescence) was determined using Adobe Photoshop CS2 version 9.0 (Adobe Inc, San Jose, California) to create 2 layers: 1 for collagen and 1 for actin. Images were analyzed in a blinded fashion by giving random numbers before analysis. Areas occupied by different colors, representing all pixels in each area, were then calculated using the CellProfiler analysis software.

Nuclei Deposition Quantification

Counting nuclei stained with DAPI was performed using the CellProfiler analysis software, where images were converted to gray, after which nuclei from different sections were counted and the average number was calculated to represent 1 BET. Manual counting was also performed to replicate and confirm the results.

Statistical Analysis

Data are shown as mean (standard error of the mean) for all groups and were compared by either *t* test, when comparing 2 variables, or 1-way analysis of variance using post hoc Dunnett tests (Prism 4.03, GraphPad Software, Inc) when comparing more than 2 variables. Group means with $P < .05$ and 95% CI determined by *t* test or analysis of variance were considered to be statistically significant.

Results

Effects of MFR on Wound Healing

Using a circular cutting apparatus, the resulting wound took on an elliptical shape immediately after wounding and continued to shape change after MFR treatment (day 0) and continuously 6 days thereafter (Fig 1A). Both the wound area and the wound minor axis showed significant decreases over time in MFR-treated BETs as compared with NS control BETs. The reductions

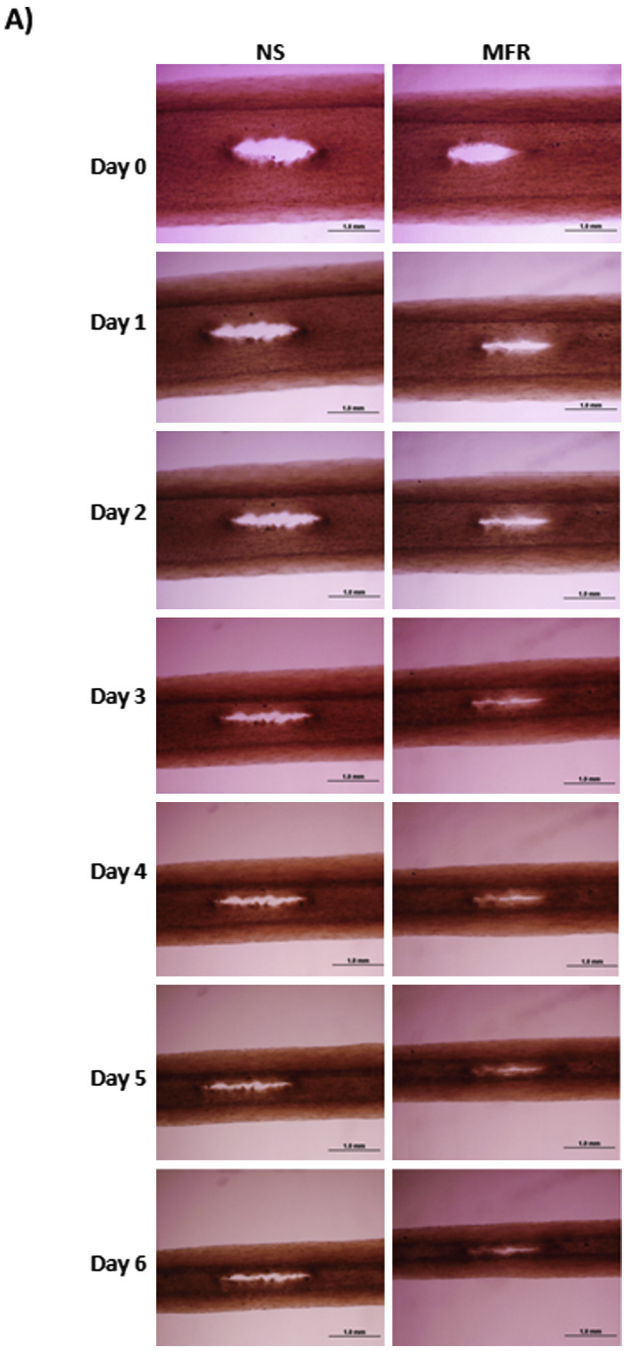

Fig 1. *Myofascial release (MFR) treatment improves wound healing of BETs. (A) Representative images of control NS and MFR-strained BETs showing enhanced wound healing in the MFR group. Scale bars: 1.0 mm. (Figure continued on next page.)*

in wound area and minor axis length were measured as a percent change from the day of wounding and MFR (day 0) and daily until day 6 (Fig 1B and C). Moreover, the thickness of BETs, when measured centrally, was significantly reduced in both MFR-strained and NS BETs. However, no changes in BETs thickness or width were observed when comparing strained with NS (Fig 1D). Measurement of the major axis in both MFR-treated BETs and NS BETs were not significantly different (Fig 1E). The latter is in agreement with our previous study, where major changes were restricted to minor axis and wound size over time.[8]

Effect of MFR on Collagen Density and Nuclei Deposition at Wound Site

Owing to the significant difference in both wound size and minor axis between MFR-strained and NS BETs, we

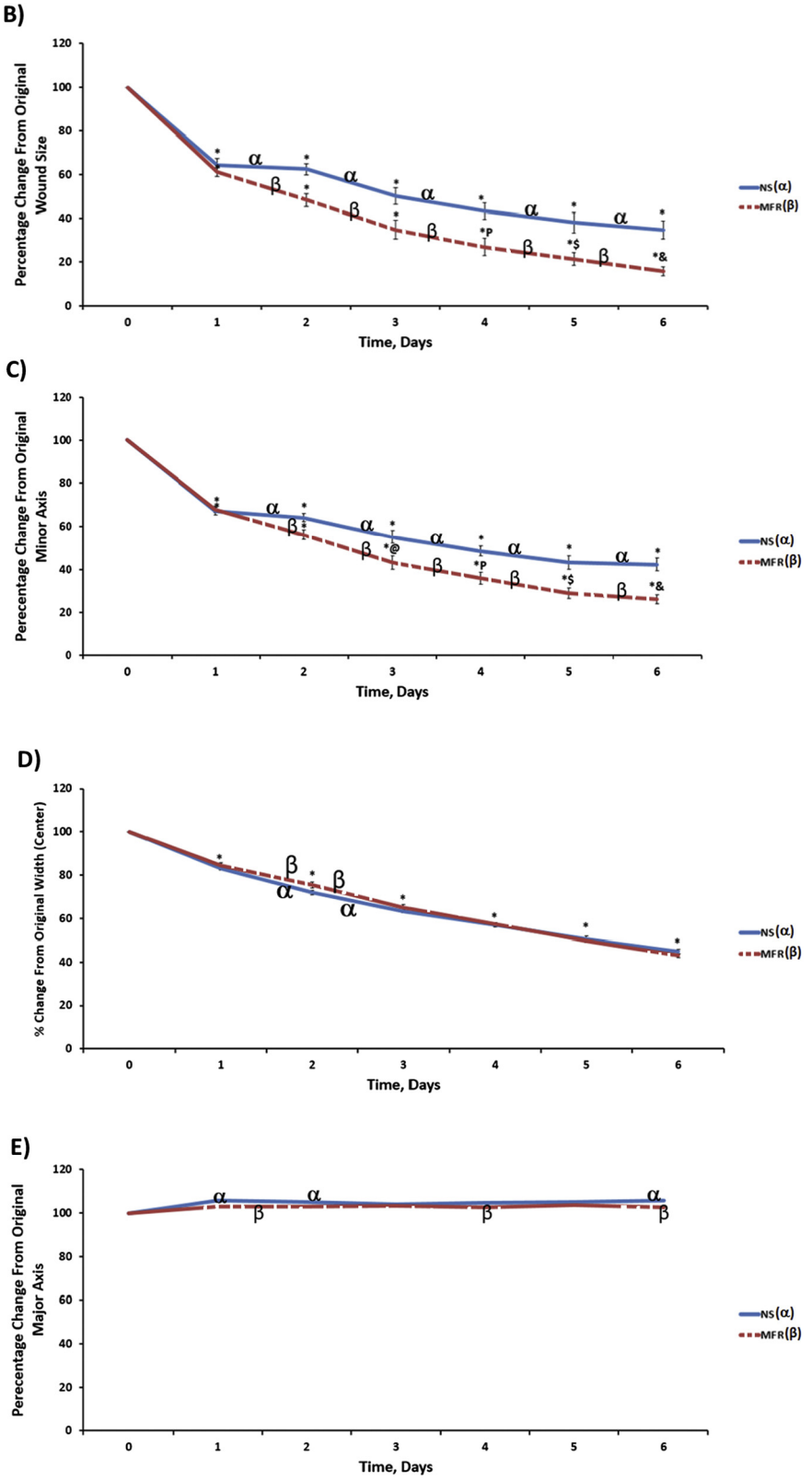

Fig 1. *(Continued from previous page.) (B, C, D, E) Changes in wound size, minor axis, major axis, and BET width measured as a percent change from day 0 (100%) daily for 6 days after MFR (symbolized by "β") treatment versus NS (symbolized by "α") (n = 11). Data are shown as mean ± standard error of the mean. *Statistically significant decrease (1-way analysis of variance, P < .05, 95% confidence interval) compared to day 0. @,P,$,&Statistically significant decrease compared to NS BETs at days 3, 4, 5, and 6, respectively.* BET, *bioengineered tendons;* NS, *nonstrained.*

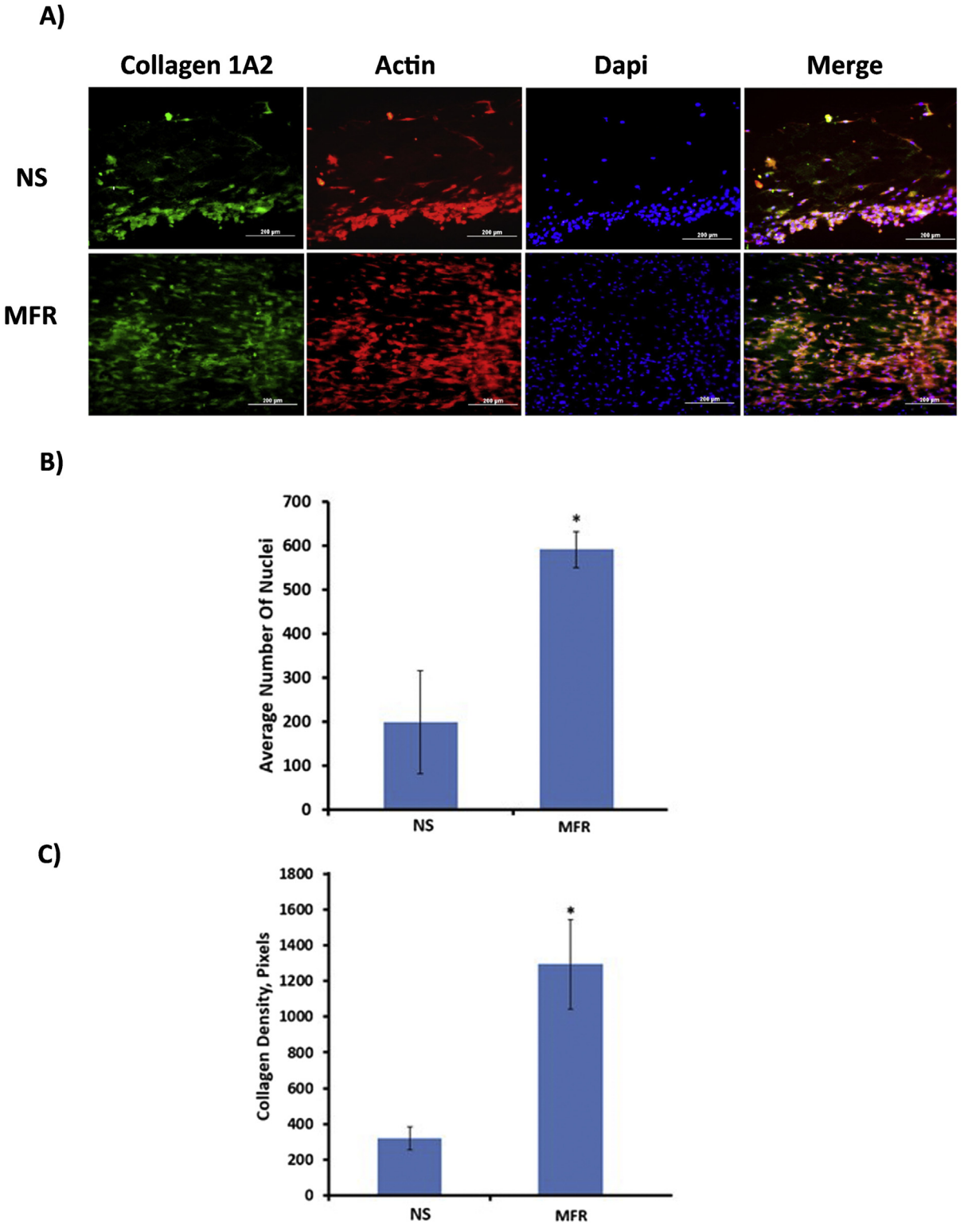

Fig 2. *Myofascial release (MFR) treatment leads to increased collagen 1A2 staining and average number of nuclei around the wound area. (A) Representative immunofluorescence images of 15 μm sections of NS and MFR-strained BETs stained with human collagen (Collagen 1A2 isoform), actin, DAPI, and merge (overlay) at day 6 after wounding and straining. Scale bar: 200 uM. (B) Average number of nuclei around the wound area 6 days after MFR treatment in BETs (n = 5-6). (C) Collagen density measured 6 days after MFR treatment in BETs (n = 4-5). Data are given as mean ± standard error of the mean. *Statistically significant decrease (*t *test, $P < .05$, 95% confidence interval) in average number of nuclei and in collagen density compared to NS.* BETs, *bioengineered tendons;* NS, *nonstrained.*

investigated the microstructure of the BETs 6 days after wounding and MFR treatment. Our results showed a significant increase in collagen density and average number of nuclei in the vicinity of the wound in MFR-strained BETs compared with NS BETs (Fig 2). When comparing changes in collagen density versus changes in average number of nuclei, we observed about a 3-times increase in the average number of nuclei in MFR-treated BETs compared with NS BETs; however, the increase in collagen density was more than 4 times as great, suggesting a nonparallel relationship in the pattern of change in cell number and collagen secretion (Fig 2B and C).

Effect of Fibroblasts on MFR-Driven Wound Healing

Our previous study showed that the presence of fibroblasts dictated the overall structural integrity of BETs. Collagen gel constructs grown in the presence of fibroblasts showed a gradual reduction in width over time, and these BETs exhibited a greater tensile strength. Fibroblast-free BETs appeared less defined and more gelatinous in structure and exhibited very low tensile strength compared with fibroblast containing BETs.[8] In the current study, we engineered fibroblast-containing BETs; however, we cultured 1 group in 0.2% FBS instead of the typical 2% FBS in order to growth arrest the cells in G_0 phase of the cell cycle. Trypan blue exclusion measurements confirmed that despite being growth arrested, 99% of the fibroblasts were viable. Our results additionally showed a 40% to 44% reduction in the number of cells surrounding the wound sites when BETs were cultured in 0.2% FBS compared to BETs cultured in 2% FBS. Such reduction was significant in all MFR-treated and NS BETs. After 6 days of MFR treatment, measurements of wound size, minor axis, major axis, and BET width showed no significant differences between MFR-treated and NS BETs when both were growth arrested (Fig 3).

Effect of Fibroblasts on Collagen Secretion and Nuclei Count in MFR-Treated BETs

After 6 days of wounding and MFR treatment, both control and MFR-treated BETs cultured in 2% FBS and 0.2% FBS were frozen and longitudinal sections were used for collagen assessment. Total collagen (bovine present in PureCol plus human fibroblast-derived) was assessed using Gomori's Trichrome stain, whereas human collagen type 1A2 was assessed using immunofluorescence. Results showed that growth-arrested fibroblasts displayed decreased staining of both total and human collagen as well as reduced nuclei deposition around the wound area (Figs 4A and 5A). Quantification of both total and human collagen showed significant increases in MFR-treated BETs when cultured in 2% FBS compared to NS BETs. Such an effect was not observed when BETs were cultured in 0.2% FBS, showing that growth-arresting fibroblasts significantly attenuated collagen secretion and blunted the effects of MFR treatment on wound healing dynamics (Figs 4B and 5B). Similarly, the average density of nuclei was significantly higher in MFR-treated BETs cultured in 2% FBS compared to NS BETs, an effect that was not observed when BETs were cultured in 0.2 % FBS, proving that growth-arresting fibroblasts significantly and predictably decreased nuclei deposition (Figs 4C and 5C).

Discussion

Mechanisms underlining wound healing after trauma, surgery, or other disease conditions remain incompletely understood but are rooted in the processes of inflammation, angiogenesis, matrix deposition, and cell recruitment.[10,11] Fibroblasts are logical targets for mechanistic studies related to wound healing and manual medicine treatments such as MFR because they respond to mechanical stimuli and are critically involved in wound healing and inflammation.[1,2] In this study, we utilized an in vitro 3D BET model to investigate the effects of optimized modeled MFR on BET wound healing 6 days after MFR treatment and the mechanisms underlying this process. Our choice for the 3D model is based on the critical role of the 3D extracellular matrix, expressed in vivo, in regulating fibroblast proliferation, migration, differentiation, and signaling responses.[12-14] In this study, MFR treatment at 3% elongation for 5 minutes was shown to be associated with accelerated wound closure rates. Moreover, our results showed significant increases in collagen density and fibroblast proliferation in MFR-strained BETs compared with NS BETs. The results from this study provide evidence to suggest that optimized MFR treatment plays a key role in enhancing wound healing by processes including fibroblast proliferation and migration as well as collagen secretion.

In the present study, the size of the original wound varied, although the same apparatus was used to induce the wound in all BETs. Such a difference can be attributed to the density of the individual fibroblasts that can easily affect the size of the implemented wound. About 100 BETs were used in our study, and the average original wound size ranged between 0.19 and 0.3 mm^2. For this variability reason, all numbers were normalized to control (day 0) represented as 100%. Our results show that the minor axis was significantly reduced 6 days after wounding and MFR treatment. In agreement with our previous study, the major axis did not show significant changes between strained and NS BETs.[8] Moreover, BET thickness and width was reduced in both strained and NS by the same extent, which may be potentially explained by the tension developed by fibroblast-mediated extracellular organization and constitutive contraction over time. This fibroblast-mediated action can be explained by Petroll et al, who reported the

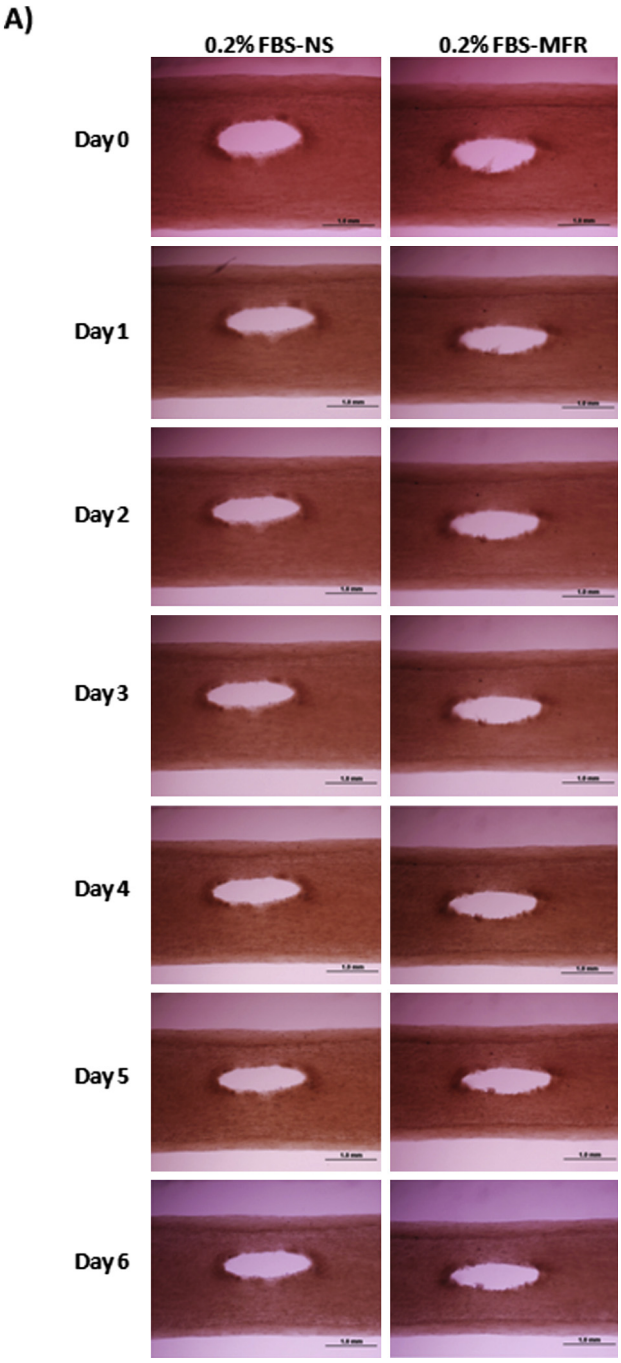

Fig 3. *Fibroblast proliferation is required for the MFR-induced wound healing. (A) Representative images of NS and MFR-strained BETs cultured with growth-arresting concentration (0.2%) FBS after wounding (day 0) and daily until day 6 after wounding and MFR. Scale bars: 1.0 mm.* *(Figure continued on next page.)*

response of corneal fibroblasts to local changes in extracellular matrix tension (ECM) and found that pulling on the ECM resulted in initial cell elongation, followed by disengagement of pseudopodia, whereas pushing the ECM toward a cell-induced contraction owing to the imbalance in the existing cellular forces, suggesting that fibroblasts respond to changes in the local matrix to maintain tensional homeostasis.[15] In agreement, Freyman et al showed that fibroblasts in attached matrices develop isometric tension.[16] Thus, we suggest that changes in BET thickness over time are caused by this tensional homeostasis. Because BET widths were not different between MFR and control groups, this suggests that this process cannot be the cause of observed differences in wound healing.

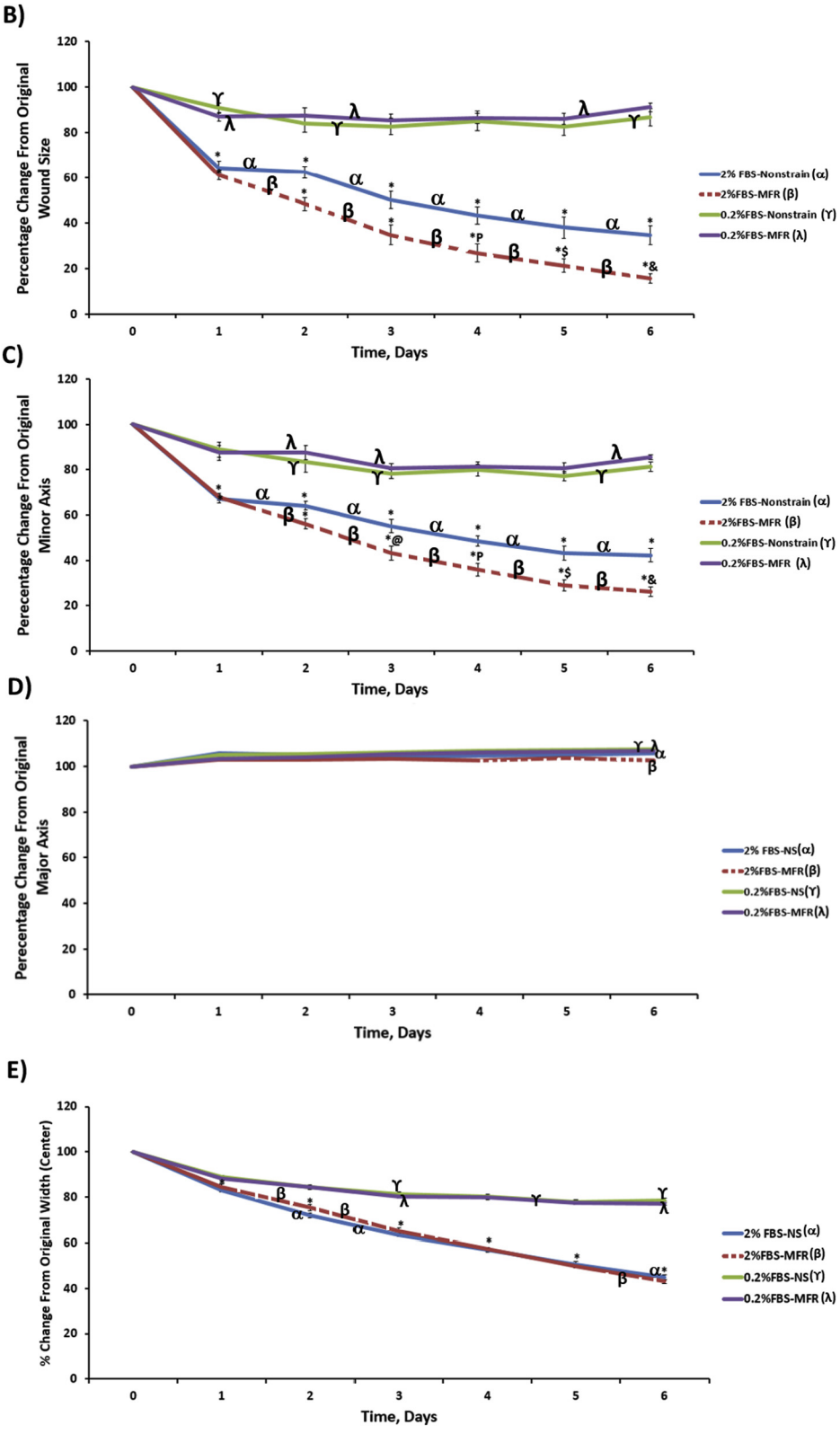

Fig 3. *(Continued from previous page.) (B, C, D, E) Change in wound size, minor axis, major axis, and BET width measured as a percent change from day 0 (100%) daily for 6 days after MFR treatment in BETs cultured with 2% FBS (n = 11) and 0.2% FBS (n = 6) (2% FBS-NS symbolized by α, 2% FBS-MFR symbolized by β, 0.2% FBS-NS symbolized by Υ, 0.2% FBS-MFR symbolized by λ). Data are given as mean ± SEM. *Statistically significant decrease (1-way analysis of variance, P < .05, 95% confidence interval) compared to day 0. $^{@,P,\$,\&}$Statistically significant decrease compared to 2% FBS cultured NS BETs at days 3, 4, 5 and 6, respectively.* BETs, *bioengineered tendons;* FBS, *fetal bovine serum;* MFR, *myofascial release;* NS, *nonstrained.*

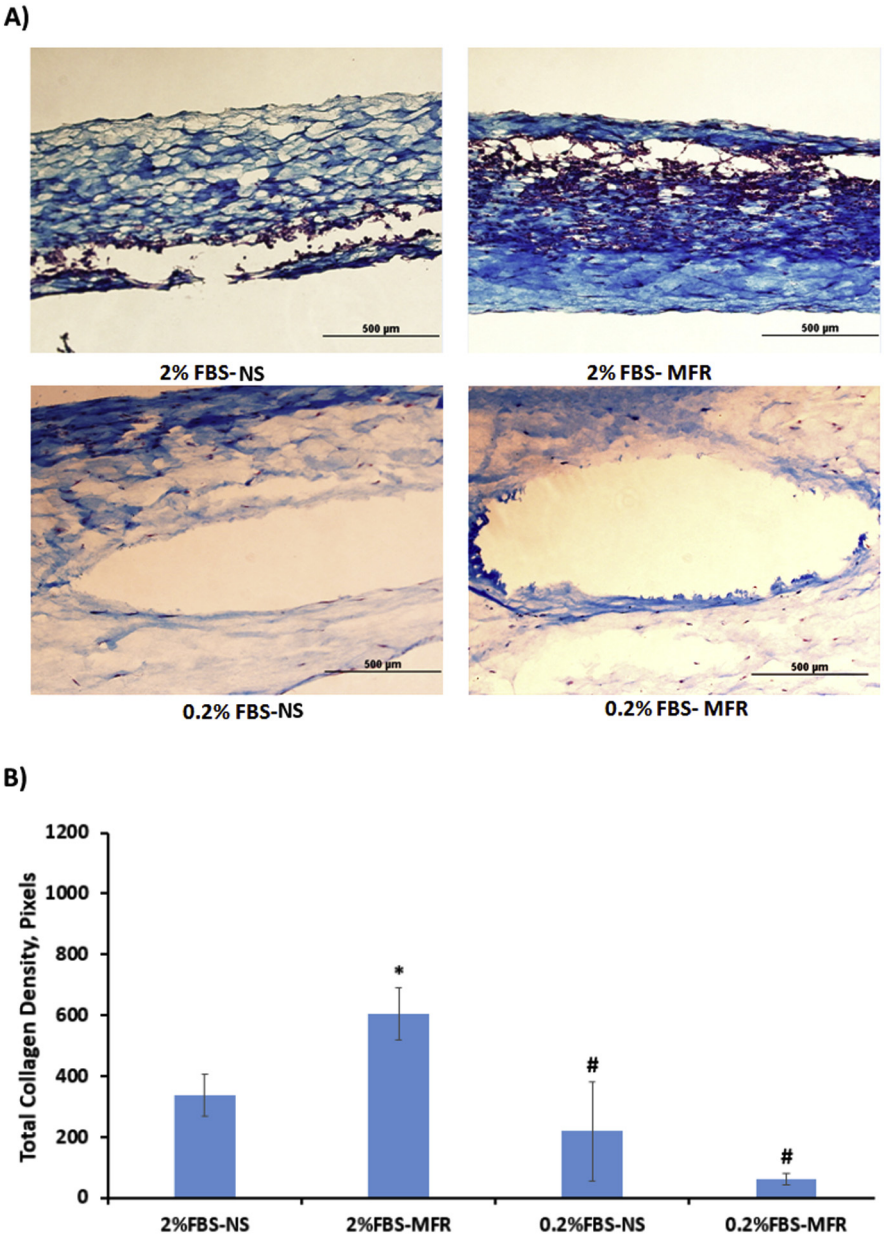

Fig 4. *Inhibition of fibroblast proliferation leads to decreased total collagen and nuclei deposition around the wound area in BETs. (A) Representative Gomori staining for collagen around the wound area in 15-µm sections of NS and MFR-strained BETs cultured with 2% and 0.2% FBS. Scale bar: 500 uM. (B) Total collagen (human and bovine) density 6 days after MFR treatment in BETs (n = 3-7).* *(Figure continued on next page.)*

Growth-arresting fibroblast was our next step to provide evidence of fibroblast proliferation involvement in the wound closure process. Our results showed that wound size, minor axis, major axis, and BET width showed no significant differences between MFR-treated and NS BETs when fibroblasts were growth arrested. This suggests that the presence of proliferating fibroblasts is critical for all observed changes in MFR-treated BETs compared with NS BETs when cultured in 2% FBS. The latter might be also correlated to BET width, in which changes might be caused by a physiological mechanism driven by fibroblasts, which when growth arrested, prevented tension development and reduction in width. These data suggest that proliferating fibroblasts are required to close the wound (a process affected by MFR) and are also required for BETs to generally develop tension (an MFR-independent process). In conclusion, MFR has specifically affected wound size but not the width and, presumably, the tension of BETs. In light of this, Darby et al reviewed the importance of fibroblasts in maintaining skin homeostasis and performing tissue repair. By interacting with

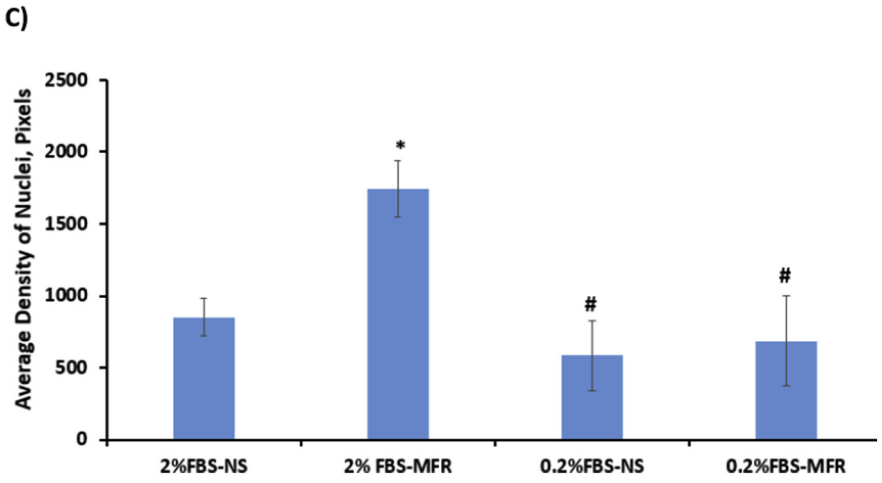

Fig 4. *(Continued from previous page.) (C) Average density of nuclei 6 days after MFR treatment in BETs (n = 3-7). Data are shown as mean ± standard error of the mean. *Statistically significant decrease (1-way analysis of variance, P < .05, 95% confidence interval) compared 2% FBS-NS. #Statistically significant decrease compared to 2% FBS-MFR cultured BETs.* BETs, *bioengineered tendons;* FBS, *fetal bovine serum;* MFR, *myofascial release;* NS, *nonstrained.*

their environment, fibroblasts form a network during wound repair, leading to a variety of processes including differentiation, proliferation, and apoptosis. Such network formation is possibly altered by certain pathological situations such as fibrosis, scarring, or aging, leading to delayed or defective wound repair process.[17] According to Singer and Clark, the course of wound healing occurs over 3 phases: the inflammatory phase, the proliferative phase, and the regeneration phase.[18] The proliferative phase is critical for the wound healing process because it allows new capillaries to deliver nutrients to the wound and contributes to the proliferation of fibroblasts. It is also known that the wound is initially hypoxic owing to lack of vascular perfusion. As fibroblasts proliferate, blood flow increases to the wound area, which subsequently develops new blood vessels and helps in the healing process.[19] Given that our in vitro BET model is devoid of capillaries, it is likely than the proliferative requirement of fibroblasts provides other key physiological processes required for wound healing independent of those related to organisms.

In collagen assessment, quantification for both total collagen and human collagen showed a significant increase in MFR-treated BETs when cultured in 2% FBS compared with NS BETs, which was not observed in growth-arrested BETs. The average density of nuclei was significantly higher in MFR-treated BETs cultured in 2% FBS compared with NS BETs, which also was not observed in growth-arrested BETs. These results suggest that inhibiting growth of fibroblasts, including their usual hyperplastic responses, significantly attenuated collagen secretion as well as nuclei deposition and thus inhibited the effect of MFR treatment. When comparing changes in collagen density to fibroblast proliferation, we observed about a 3-times increase in the average number of nuclei in MFR-treated compared with NS BETs, whereas the increase in collagen density was more than 4 times, suggesting a nonparallel relationship in the pattern of change in cell number and collagen secretion. One possible explanation can be linked to the possibility that MFR has stimulated some resident population of fibroblasts to secrete more collagen in addition to the observed increase in proliferation of cells. Kanta reviewed the interaction between fibroblast and collagen. When fibroblasts are activated around the wound area, they migrate to the matrix that contains fibrin and fibronectin, where fibrin mediates fibroblast and inflammatory cell migration to the wound area.[20] Afterward, fibroblasts begin secreting collagen and the matrix becomes replaced with a collagenous ECM.[20] Additionally, fibroblasts have the tendency to aggregate on collagen gel and when fibroblasts are embedded in collagen, they remodel the surrounding matrix.[21,22] Researchers also showed that increase collagen concentration supports cell proliferation and prevents apoptosis[23] and that fibroblasts are affected by intrinsic forces produced by the ECM and extracellular fluid.[24] Consequently, we believe that our data are consistent with concomitant fibroblast proliferation and collagen secretion playing critical roles to expedite the wound healing process after FR. When one factor is inhibited (eg, fibroblast proliferation), the other factor (collagen secretion) will be affected, which ultimately will disturb the process of wound healing. Our results from these experiments suggest an upregulation of collagen secretion and an increase in nuclei deposition owing to increased fibroblast proliferation, and likely migration, driven by MFR. Another explanation that we have not ruled out yet is reorganization of bovine collagen that

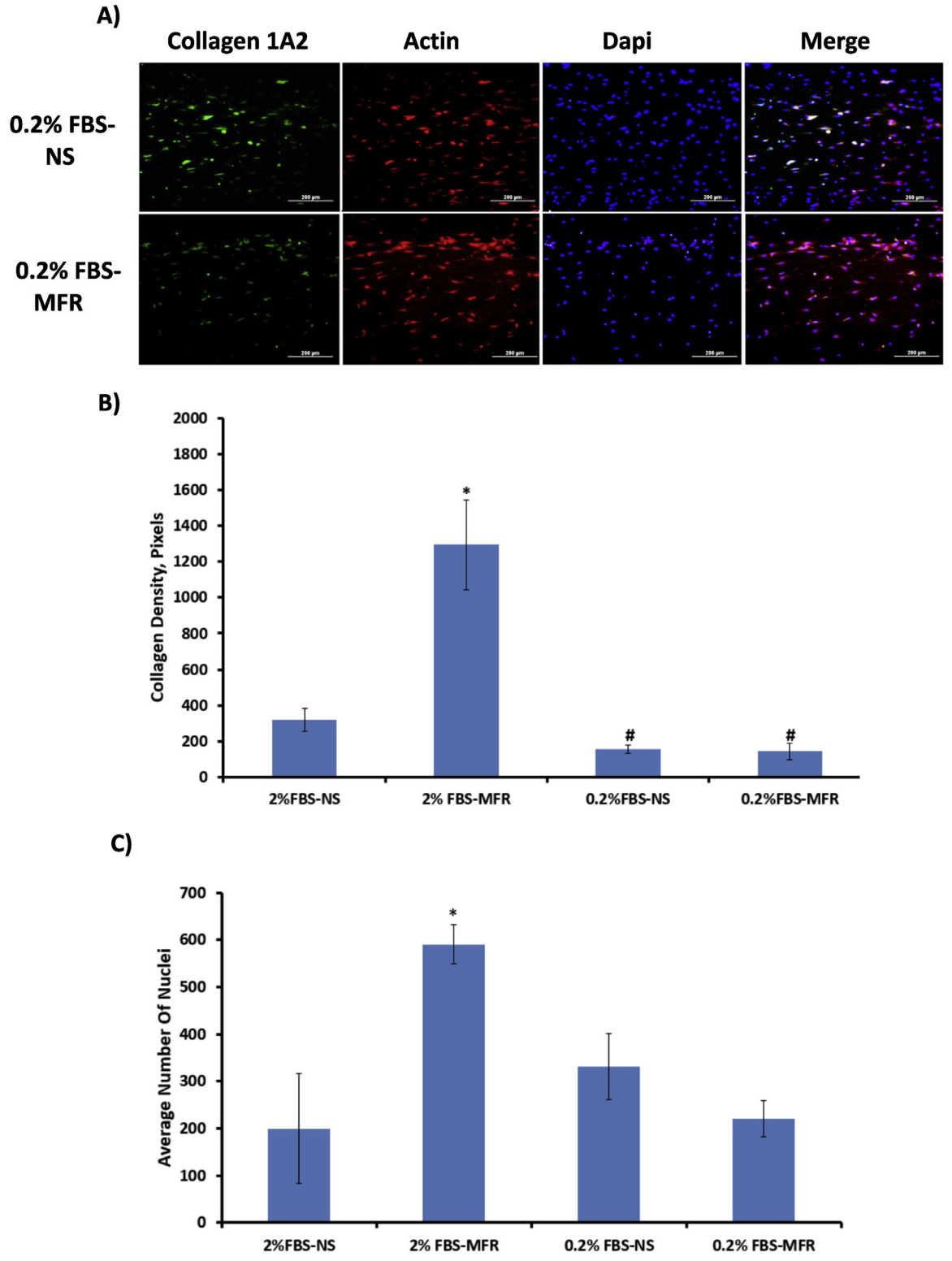

Fig 5. *Inhibition of fibroblast proliferation leads to decreased human collagen and nuclei deposition around the wound area in BETs. (A) Representative immunofluorescence images of 15-μm sections of NS and MFR-strained BETs cultured with 0.2% FBS and stained with human collagen (Collagen 1A2 isoform), actin, DAPI, and merge (overlay) at day 6 after wounding and straining. Scale bar: 200 uM. (B) Human collagen density 6 days after MFR treatment in BETs cultured with 2% FBS and 0.2% FBS (n = 3-5). (C) Average number of nuclei around the wound area 6 days after MFR treatment in BETs cultured with 2% FBS and 0.2% FBS (n = 3-6). Data are shown as mean ± standard error of the mean. *Statistically significant decrease (1-way analysis of variance, P < .05, 95% confidence interval) compared 2% FBS-NS. #Statistically significant decrease compared to 2% FBS-MFR cultured BETs.* BETs, *bioengineered tendons;* FBS, *fetal bovine serum;* MFR, *myofascial release;* NS, *nonstrained.*

was used for fabricating BETs because Gomori staining density is greater in the wound area after MFR. The exact contribution of this reorganization versus new synthesis of fibroblast-derived collagen is an area we are currently investigating. If clinically translatable, our results support a likely mechanism by which optimized MFR improves wound healing and consequent tissue performance.

Limitations

A limitation of this study was the use of in vitro models. These models lack blood, tissue fluid dynamics, and other cells that contribute to inflammation and wound healing. Other factors were not included, like age and other patient-related physical variations, which may also play a role in the response to the myofascial treatment applied by the physician in a clinical setting. Using our in vitro model, we did negate the effects of age and tissue integrity in addition to external environmental factors. All these factors were beyond the scope of this study.

Future Studies

Our next step should focus more on inhibiting both fibroblast proliferation and migration, a step that, we believe, is critical for further emphasizing the role of fibroblasts in wound healing. Future studies should include implementing inhibitors of fibroblast migration and proliferation and determining if MFR effects are observed. Additionally, using a human-specific collagen antibody, we will determine if new fibroblast-derived collagen production accounts for MFR-induced hastening of wound healing.

Conclusion

We found that optimized MFR results in improved wound healing owing to increased fibroblast deposition and collagen density within and adjacent to the wound area. Such effects are impaired in growth-arrested BETs, thus proving the requirement of actively proliferating fibroblasts. A portion of wound healing impairment may be correlated to loss of human fibroblast collagen secretion and integration into the ECM.

Funding Sources and Conflicts of Interest

This study was supported by the American Osteopathic Association (Grant 1121640) and the University of Arizona, College of Medicine-Phoenix. No conflicts of interest were reported for this study.

Contributorship Information

Concept development (provided idea for the research): P.R.S.

Design (planned the methods to generate the results): M.Z.-H.

Supervision (provided oversight, responsible for organization and implementation, writing of the manuscript): P.R.S.

Data collection/processing (responsible for experiments, organization, or reporting data): M.Z.-H.

Analysis/interpretation (responsible for statistical analysis, evaluation, and presentation of the results): M.Z.-H.

Literature search (performed the literature search): M.Z.-H.

Writing (responsible for writing a substantive part of the manuscript): M.Z.-H.

Critical review (revised manuscript for intellectual content, this does not relate to spelling and grammar checking): P.R.S.

Practical Applications

- The findings of this study suggest that optimizing magnitude and duration of strain may clinically translate to optimal patient outcomes.
- Mechanical strain of fibroblasts may underlie MFR's clinical efficacy.
- Myofascial release may enhance wound healing clinical via fibroblast actions.

References

1. Meltzer KR, Cao TV, Schad JF, King H, Stoll ST, Standley PR. In vitro modeling of repetitive motion injury and myofascial release. *J Bodyw Mov Ther*. 2010;14(2):162-171.
2. Meltzer KR, Standley PR. Modeled repetitive motion strain and indirect osteopathic manipulative techniques in regulation of human fibroblast proliferation and interleukin secretion. *J Am Osteopath Assoc*. 2007;107(12):527-536.
3. Sucher BM. Myofascial manipulative release of carpal tunnel syndrome: documentation with magnetic resonance imaging. *J Am Osteopath Assoc*. 1993;93(12):1273-1278.
4. Hanten WP, Chandler SD. Effects of myofascial release leg pull and sagittal plane isometric contract-relax techniques on passive straight-leg raise angle. *J Orthop Sports Phys Ther*. 1994;20(3):138-144.
5. Buckley CD, Pilling D, Lord JM, Akbar AN, Scheel-Toellner D, Salmon M. Fibroblasts regulate the switch from acute resolving to chronic persistent inflammation. *Trends Immunol*. 2001;22(4):199-204.
6. Hicks MR, Cao TV, Campbell DH, Standley PR. Mechanical strain applied to human fibroblasts differentially regulates skeletal myoblast differentiation. *J Appl Physiol (1985)*. 2012;113(3):465-472.
7. Eagan TS, Meltzer KR, Standley PR. Importance of strain direction in regulating human fibroblast proliferation and

cytokine secretion: a useful in vitro model for soft tissue injury and manual medicine treatments. *J Manipulative Physiol Ther*. 2007;30(8):584-592.
8. Cao TV, Hicks MR, Zein-Hammoud M, Standley PR. Duration and magnitude of myofascial release in 3-dimensional bioengineered tendons: effects on wound healing. *J Am Osteopath Assoc*. 2015;115(2):72-82.
9. Grinnell F. Fibroblast biology in three-dimensional collagen matrices. *Trends Cell Biol*. 2003;13(5):264-269.
10. Eming SA, Martin P, Tomic-Canic M. Wound repair and regeneration: mechanisms, signaling, and translation. *Sci Transl Med*. 2014;6(265):265sr6.
11. Reish R, Eriksson E. Scars: a review of emerging and currently available therapies. *Plast Reconstr Surg*. 2008; 122(4):1068-1078.
12. Mio T, Adachi Y, Romberger DJ, Ertl RF, Rennard SI. Regulation of fibroblast proliferation in three-dimensional collagen gel matrix. *In Vitro Cell Dev Biol Anim*. 1996;32(7):427-433.
13. Green JA, Yamada KM. Three-dimensional microenvironments modulate fibroblast signaling responses. *Adv Drug Deliv Rev*. 2007;59(13):1293-1298.
14. Paszek MJ, Zahir N, Johnson KR, et al. Tensional homeostasis and the malignant phenotype. *Cancer Cell*. 2005;8(3):241-254.
15. Petroll WM, Vishwanath M, Ma L. Corneal fibroblasts respond rapidly to changes in local mechanical stress. *Invest Ophthalmol Vis Sci*. 2004;45(10):3466-3474.
16. Freyman TM, Yannas IV, Yokoo R, Gibson LJ. Fibroblast contractile force is independent of the stiffness which resists the contraction. *Exp Cell Res*. 2002;272(2):153-162.
17. Darby IA, Laverdet B, Bonté F, Desmoulière A. Fibroblasts and myofibroblasts in wound healing. *Clin Cosmet Investig Dermatol*. 2014;7:301-311.
18. Singer AJ, Clark RA. Cutaneous wound healing. *N Engl J Med*. 1999;341(10):738-746.
19. Wietecha MS, DiPietro LA. Therapeutic approaches to the regulation of wound angiogenesis. *Adv Wound Care (New Rochelle)*. 2013;2(3):81-86.
20. Kanta J. Collagen matrix as a tool in studying fibroblastic cell behavior. *Cell Adhes Migr*. 2015;9(4):308-316.
21. da Rocha-Azevedo B, Grinnell F. Fibroblast morphogenesis on 3D collagen matrices: the balance between cell clustering and cell migration. *Exp Cell Res*. 2013;319(16): 2440-2446.
22. Jiroutova A, Peterová E, Bittnerová L, et al. Collagenolytic potential of rat liver myofibroblasts. *Physiol Res*. 2013;62(1): 15-25.
23. Helary C, Zarka M, Giraud-Guille MM. Fibroblasts within concentrated collagen hydrogels favour chronic skin wound healing. *J Tissue Eng Regen Med*. 2012;6(3):225-237.
24. Agha R, Ogawa R, Pietramaggiori G, et al. A review of the role of mechanical forces in cutaneous wound healing. *J Surg Res*. 2011;171(2):700-708.